Chemical and Process Engineering Research
ISSN 2224-7467 (Paper) ISSN 2225-0913 (Online)
Vol.42, 2016

Homogeneous/heterogeneous reactions of the water based Cu, Al_2O_3 and SWCNTs on MHD Stagnation-point flow over stretching/shrinking sheet with generalized slip condition

Radiah Mohammad and R. Kandasamy
Research Centre for Computational Mathematics, FSTPi, Universiti Tun Hussein Onn Malaysia, 86400, Parit Raja, Batu Pahat, Johor, Malaysia

Abstract
An investigation is performed to analyze thehomogeneous–heterogeneous reactions of water based Cu, Al_2O_3 and SWCNTs on MHD stagnation-point over a permeable stretching/shrinking sheet with generalized slip condition. In this study we employed the refined model of a homogeneous–heterogeneous reaction in boundary layer nanofluid flow with equal diffusivities for reactant and autocatalysis. The governing PDEs in terms of continuity, momentum and concentration are transformed into ODEs and then solved numerically using fourth or fifth order Runge-Kutta Fehlberg method with shooting technique. The results show that for the shrinking sheet, the concentration of SWCNTs-water of heterogeneous reaction is stronger as compare with homogeneous reaction. Comparison of the present results with previously published work is given and found in good agreement.
Keywords: Stagnation point flow, Nanofluids, Homogeneous-heterogeneous reaction, Shrinking sheet, SWCNTs-water, Slip condition.

1. Introduction

The study of the stagnation-point flow of a viscous fluid over a stretching/shrinking sheet has gained attention of many researchers due to its wide range of applications in many industrial manufacturing processes. These processes include glass blowing, aerodynamic extrusion of plastic sheet, continuous casting and spinning of fibers, the cooling and drying of papers and textiles, etc. Hiemenz [1], Paullet and Weidman [2],Sharma and Singh [3], Ishak et al. [4], Hayat et al. [5], Ali et al. [6], Subhashini et al. [7], Bhattacharyya et al. [8] and Al-Sudais [9]. Additionally, it is noted that flow due to a shrinking sheet was studied by Miklavčič and Wang [10], Wang [11], Bhattacharyya and Layek [12], Bhattacharyya and Vajravelu [13], Ashraf and Ahmad [14], Rohni et al. [15] and Saleh et al. [16]. It is worth mentioning here that there are two conditions for the flow of a shrinking sheet to exist, namely, whether a sufficient suction is added on the boundary (Miklavčič and Wang [10]) or a stagnation flow is considered (Wang [11]) to maintain the velocity of shrinking sheet in the boundary layer.In fluid dynamics, the no-slip condition for viscous fluids states that at a solid boundary, the fluid will have zero velocity relative to the boundary,but in slip flow, the flow velocity is non-zero at the solid wall, Navier [17], Maxwell [18], Wang [19], Thompson and Troian [20], Mathews and Hill [21], Wang [22]and Sajid et al. [23].

Chemical reactions can be classified as either homogeneous or heterogeneous process depending on whether they occur in bulk of the fluid (homogeneous) or occur on some catalytic surfaces (heterogeneous). Homogeneity and heterogeneity are concepts often used in the sciences and statistics relating to the uniformity in a substance or organism. A material or image that is homogeneous is uniform in composition or character (i.e. color, shape, size, weight, height, distribution, texture, language, income, disease, temperature, radioactivity, architectural design, etc.); one that is heterogeneous is distinctly non-uniform in one of these qualities, [24-26].The correlation between homogeneous and heterogeneous reactions associated with formation and consumption of reactant species at different rates both within the fluid and on the catalytic surfaces is usually very complex, Chaudhary and Merkin [27–29], Merkin [30], Khan and Pop [31], Bachok et al. [32], Khan and Pop [33] and Kameswaran et al. [34]. Moreover, Kameswaran et al. [35] analyzed the impact of homogeneous–heterogeneous reactions over a stretching sheet in a porous medium saturated with a nanofluid. Shaw et al. [36] investigated the role of homogeneous–heterogeneous reactions on a boundary layer flow of a micropolar fluid over a permeable stretching/shrinking sheet in a porous medium.

Suspended nanoparticles in conventional fluids, called nanofluids, have been the subject of intensive study worldwide since pioneering researchers recently discovered the anomalous thermal behavior of these fluids. The enhanced thermal conductivity of these fluids with small-particle concentration was surprising and could not be explained by existing theories. Micrometer-sized particle-fluid suspensions exhibit no such dramatic

enhancement. Liu et al. [37], Ahuja [38] and Eastman et al., [39] investigated that the fluids with suspended large particles have little practical application in heat transfer enhancement.Some researchers tried to suspend nanoparticles into fluids to form high effective heat transfer fluids. Choi [40] is the first who used the term nanofluids to refer to the fluids with suspended nanoparticles. By suspending nanophase particles in heating or cooling fluids, the heat transfer performance of the fluid can be significantly improved. The vital reasons may be indexed as follows: (i) thesuspended nanoparticles enhance the surface area and the heat capacity of the fluid. (ii) the suspended nanoparticles raise the effective (or apparent) thermal conductivity of the fluid. (iii) the interaction and collision among particles, fluid and the flow passage surface are intensified. (iv)the dispersion of nanoparticles flattens the transverse temperature gradient of the fluid.

The most important feature observed in nanofluids was an abnormal rise in thermal conductivity, far beyond expectations and much higher than any theory could predict. Nanofluids have been reported to be stable over months using a stabilizing agent [41, 42]. Bhattacharya et al. [43] also investigated that the Brownian dynamics simulation to determine the effective conductivity of nanofluids. The simulation results were within 3% of experimental data for Al_2O_3–ethylene glycol and in nearly full agreement with Cu–ethylene glycol. Recently, Xuan and Yao [44] developed a Lattice Boltzmann model to investigate nanoparticle distribution and flow pattern and found that the main flow and rising temperature of the fluid can improve nanoparticle distribution, which is beneficial to energy transport enhancement of the nanofluids. Nan et al. [45] have presented a simple formula for thermal conductivity enhancement in CNT composites that is derived from the Maxwell-Garnett model [46] by the effective medium approach. The model over predicts the enhancement in the thermal conductivity of CNT suspensions when calculated with typical values of CNT thermal conductivities. The same authors have also developed a new model [47] by incorporating interface thermal resistance with an effective medium approach. However, the model needs the thermal resistance value at the surface of CNTs, which is difficult to get for different types of CNTs and their combinations with different solvents. The researchers, led by Sivasankaran Harish et al. [48] found that their single-walled carbon nanotube (SWCNT) nanofluid exhibits an increase in conductivity of up to almost 15%; a value significantly higher than what has been achieved with nanoparticle-based nanofluids.

The purpose of the current investigation is to study the effects of the water based Cu, Al_2O_3 and SWCNTs on MHD stagnation-point flow over a permeable stretching/shrinking sheet with homogeneous–heterogeneous reactions and generalized slip at the boundary. Numerical and analytical solution of transformed similarity equations are obtained for both stretching and shrinking sheet in terms of velocity and concentration profiles for several values of the governing parameters. The physical significance of the controlling nanofluid (water based Cu, Al_2O_3 and SWCNTs) parameters on the flow field and concentration profiles are analyzed graphically.

2. Mathematical analysis

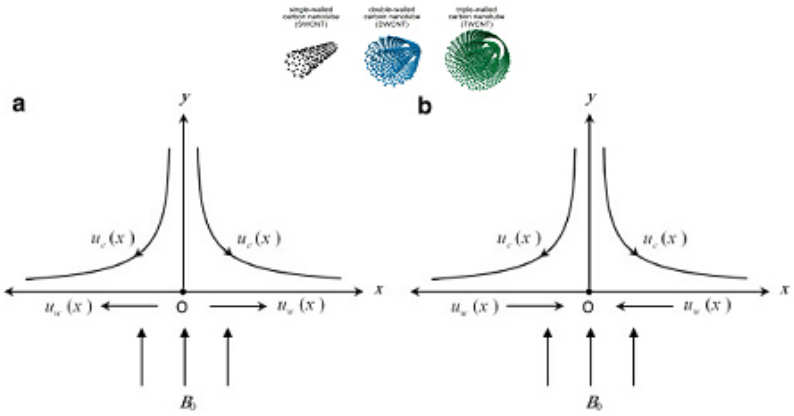

Fig. 1: Physical significance of (a) stretching sheet and (b) shrinking sheet [49]

We consider the steady two-dimensional MHD stagnation-point flow of an incompressible water based Cu, Al_2O_3 and SWCNTs over a horizontal linearly stretching/shrinking sheet in its own plane with a velocity proportional to the distance from the stagnation-point. The sheet is in the plane $y = 0$ and the stretched/shrunk

sheet is in the x - direction with the velocity varying linearly along it ie. $u_w(x) = mx$, where $m > 0$ is for the stretching sheet, $m = 0$ is for the static sheet and $m < 0$ is for the shrinking sheet, respectively. The free stream velocity is assumed as $u_e(x) = cx$,where $c > 0$ is the strength of the stagnation-point flow. A uniform external magnetic field of strength B_0 is applied normal to the stretching/shrinking surface. Under the assumption of small magnetic Reynolds number, the induced magnetic field is negligible and external electric field is zero. We also assume a simple model for the interaction between a homogeneous (or bulk) and heterogeneous (on sheet) reactions involving the two chemical species A and B in a boundary layer flow as stated by Chaudhary and Merkin [29] and Merkin [30]:

$$A + 2B \to 3B, \ rate = K_h\, ab^2, \tag{1}$$

$$A \to B, rate = K_s a \tag{2}$$

a and b are the concentrations of the chemical species A and B, respectively whereas K_h and K_s are the rate of homogeneous and heterogeneous reactant. It is expected that both reaction processes are isothermal and far away from the sheet at the ambient fluid, there is a uniform concentration a_0 of reactant A and there is no auto catalyst in reactant B. Under the boundary layer approximations and all the above mentioned assumptions, the governing equations can be written as:

$$\frac{\partial u}{\partial x} + \frac{\partial v}{\partial y} = 0 \tag{3}$$

$$\rho_{nf}\left(u\frac{\partial u}{\partial x} + v\frac{\partial u}{\partial y}\right) = u_e\frac{du_e}{dx} + \mu_{f_n}\frac{\partial^2 u}{\partial y^2} - \sigma_{nf}B_o^2(u - u_e) \tag{4}$$

$$u\frac{\partial a}{\partial x} + v\frac{\partial a}{\partial y} = (D_A)_{nf}\left(\frac{\partial^2 a}{\partial y^2} - K_h ab^2\right) \tag{5}$$

$$u\frac{\partial b}{\partial x} + v\frac{\partial b}{\partial y} = (D_B)_{nf}\left(\frac{\partial^2 b}{\partial y^2} + K_h ab^2\right) \tag{6}$$

u and v - the velocity components in x and y directions, ν_f - kinematic viscosity of the base fluid, σ_{nf} - electrical conductivity of the nanofluid and, $(D_A)_{nf}$ and $(D_B)_{nf}$ - diffusion coefficients of nanofluid. Following Thompson and Troian [20], we assume generalized slip boundary condition by the relation

$$u_t = \alpha^*(1 - \beta^*\tau_w)^{-0.5}\tau_w \tag{7}$$

u_t - tangential velocity, α^* -Navier's constant slip length, β^* - reciprocal of some critical shear rate and τ_w - shear rate at the wall. The boundary conditions for the problem under consideration are

$$u(0) = u_w(x) = mx + \alpha^*(1 - \beta^*\frac{\partial u}{\partial y})^{-0.5}\frac{\partial u}{\partial y}, v(0) = -v_w(x), u(\infty) = u_e(x) = cx,$$

$$(D_A)_f\left.\frac{\partial a}{\partial y}\right|_{y=0} = K_s a(0), (D_B)_f\left.\frac{\partial b}{\partial y}\right|_{y=0} = -K_s a(0), a(\infty) = a_0, b(\infty) = 0 \tag{8}$$

m and c - constants having dimension $(time)^{-1}, v_w > 0$ - constant mass transfer (suction) velocity and a_0 - constant. ρ_{nf} - effective density of the nanofluid, μ_{nf} - effective dynamic viscosity of the nanofluid and D_{nf} - mass diffusivity of the nanofluid are defined by Magyari [55] and Mamut [56] as

$$\rho_{nf}=(1-\zeta)\rho_f+\zeta\rho_s,\ \mu_{nf}=\frac{\mu_f}{(1-\zeta)^{2.5}},\ D_{nf}=(1-\zeta)D_f,\ \frac{\sigma_{nf}}{\sigma_f}=\left\{\frac{3\left(\frac{\sigma_s}{\sigma_f}-1\right)\zeta}{\left(\frac{\sigma_s}{\sigma_f}+2\right)-\left(\frac{\sigma_s}{\sigma_f}-1\right)\zeta}\right\} \quad (9)$$

ζ - Nanoparticle volume fraction, μ_f - dynamic viscosity of the base fluid, σ_f and σ_s - electrical conductivity of the base fluid and nanoparticle, ρ_f and ρ_s - density of the base fluid and nanoparticle, D_f - mass diffusivity of the nanofluid, σ_{nf} - electrical conductivity of the nanofluid.By using following similarity transformations, the governing equations take the non-dimensional form

$$\eta=\sqrt{\frac{c}{\nu_f}}y,\psi=\sqrt{c\nu_f}xf(\eta),u=cxf'(\eta),v=-\sqrt{c\nu}f(\eta),g(\eta)=\frac{a}{a_0},h(\eta)=\frac{b}{a_0} \quad (10)$$

TheEqus. (3)–(6) become

$$f'''+A1\left(f\ f''-f'^2+\frac{A2.A3}{A1}M(1-f')+1\right)=0 \quad (11)$$

$$g''+\frac{Sc}{A_4}\left(fg'-Kgh^2\right)=0 \quad (12)$$

$$h''+\frac{Sc}{A_4}\left(fh'+Kgh^2\right)=0 \quad (13)$$

subject to the boundary conditions

$$f(0)=S,f'(0)=\lambda+\alpha+\left(1-\beta(x)f''(0)\right)^{-0.5}f''(0),f'(\infty)=1$$

$$g'(0)=\frac{K_c g(0)}{A4},g(\infty)=1,\frac{D_B}{D_A}h'(0)=-\frac{K_c h(0)}{A4},h(\infty)=0, \quad (14)$$

where $A1=(1-\zeta)^{2.5}\left(1-\zeta+\zeta\frac{\rho_s}{\rho_f}\right)$, $A2=(1-\zeta)^{2.5}$, $A3=\left\{\frac{3\left(\frac{\sigma_s}{\sigma_f}-1\right)\zeta}{\left(\frac{\sigma_s}{\sigma_f}+2\right)-\left(\frac{\sigma_s}{\sigma_f}-1\right)\zeta}\right\}$, $A4=(1-\zeta)$, $M=\frac{B_0^2\sigma_f x}{\rho_f u_e}$ - magnetic parameter, $S=\frac{v_w}{\sqrt{c\nu_f}}$ - suction parameter if $S>0$, $\lambda=\frac{m}{c}$ - ratio of stretching rate to external flow rate with $\lambda>0$ for a stretching sheet, $\lambda<0$ for a shrinking sheet and $\lambda=0$ for a static sheet, $Sc=\frac{\nu_f}{D_A}$ - Schmidt number, $\delta=\frac{D_B}{D_A}$ - ratio of the diffusion coefficients, $\frac{K_h a_0^2 x}{u_e}$ - strength of the homogeneous reaction and $\frac{K_s\,\mathrm{Re}^{-0.5}}{(D_A)_f}$ - strength of heterogeneous reaction and $\mathrm{Re}=\frac{c}{\nu_f}$ - Reynolds number. In Equ. (14), α and β are the dimensionless velocity slip parameter and the dimensionless critical shear rate, which are defined as

$$\alpha=\sqrt{\frac{c}{\nu_f}}\alpha^*,\ \beta(x)=\sqrt{\frac{c}{\nu_f}}\beta^*(x)x \quad (15)$$

As it was suggested by Aziz [47], for Equs. (10)–(12) to have a similarity solution, the quantities α and β must be constants and not functions of variable x as in Equ. (15). This condition can be met if $\beta^*(x)$ is proportional to x^{-1}. We therefore assume

$$\alpha^*(x)=\alpha^*,\beta^*(x)=b^*x^{-1} \tag{16}$$

wherea^* and $b^*$are constants. With the introduction of (16) into (15), we have

$$\alpha=\sqrt{\frac{c}{\nu_f}}\alpha^*,\beta=\sqrt{\frac{c}{\nu_f}}b^* \tag{17}$$

We mention that with α and β defined by Equ.(6), the solution of Equs. (10)–(12) yield the similarity solutions. However, with α and β defined by Equ.(15), the solutions generated are the local similarity solutions.Generally, in most applications diffusion coefficients of chemical species A and B are to be of a comparable size, which undergo for further supposition that the diffusion coefficients $(D_A)_f$ and $(D_B)_f$ are equal ($\delta=1$, see [30]). As a result of this assumption, we have a following relation

$$g(\eta)+h(\eta)=1 \tag{18}$$

Therefore, Equs. (11)and (12) become

$$g''+\frac{Sc}{A_4}\left(fg'-Kg(1-g)^2\right)=0 \tag{19}$$

with boundary conditions

$$g'(0)=\frac{K_c g(0)}{A4},g(\infty)=1 \tag{20}$$

The physical quantity of interest here is the skin friction coefficient C_f and τ_w is the shear stress at the surface of the wallwhich are given by

$$C_f=\frac{\tau_w}{\rho_f u_w^2}\text{ and }\tau_w=\mu_f\left(\frac{\partial u}{\partial y}\right)_{y=0} \tag{21}$$

usingEqu. (10) we get

$$R_{ex}^{0.5}C_f=f''(0) \tag{23}$$

$R_{ex}=\frac{u_w x}{\nu_f}$ - Local Reynolds number.

3. Numerical solution

Equs. (11) and(19) subjected to the boundary condition (14) are converted into the following simultaneous system of first order differential equations as follows:

$$f'(\eta)=u(\eta)\,,u'f(\eta)=v(\eta)\,,v'(\eta)=-A1\left(f(\eta)f''(\eta)-f'^2(\eta)+\frac{A2.A3}{A1}M(1-f'(\eta))+1\right) \tag{24}$$

$$g'(\eta)=p(\eta)\,,\ p'(\eta)=-\frac{Sc}{A_4}\left(f(\eta)g'(\eta)-Kg(\eta)(1-g(\eta))^2\right) \tag{25}$$

The boundary conditions

$$f(0)=S, u(0)=\lambda+\alpha(1-\beta.\tau)^{-0.5}\tau, g(0)=\frac{A4.\gamma}{Kc}, v(0)=\tau, p(0)=\gamma, u(L)=1, g(L)=1 \qquad (26)$$

where τ and γ are priori unknowns to be determined as a part of the solution.

By using DSolve subroutine in MAPLE 18 we can get a solution for the system of Equs. (24)-(25) with conditions (26). This software uses a fourth-fifth order Runge–Kutta–Fehlberg method with shooting technique as default to solve the boundary value problems numerically using the Dsolve command. The values of τ and γ are determined upon solving the boundary conditions $v(0)=\tau, p(0)=\gamma$ with trial and error basis The numerical results are represented in the form of the dimensionless velocity and concentration in the presence of water based SWCNT, Cu and Al_2O_3.

4. Analytical solution using optimal homotopy asymptotic method (OHAM)

Based on the optimal homotopy asymptotic method, the nonlinear ordinary differential equations (11) and (19) with boundary conditions (14) can be assumed as

$f = f_0 + pf_1 + p^2 f_2$, $g = g_0 + pg_1 + p^2 g_2$, $H_1(p) = pC_1 + p^2 C_2$ and $H_2(p) = pC_3 + p^2 C_4$

where $p \in [0,1]$ is an embedding parameter, H_p is a nonzero auxiliary function, C_i are constants,Marinca and Herisanu[50].

4.1.Approximation of the momentum boundary layer problem

Based on the optimal homotopy asymptotic method, Equ. (11) and the boundary conditions (14) can be written as

$$L = f'' + f' \text{ and } N = f''' + A1\left(f\, f'' - f'^2 + \frac{A2.A3}{A1} M\,(1-f') + 1 \right) - f'' - f' \qquad (27)$$

L and N be the linear operator and the nonlinear operator. After applied OHAM to the Equ. (8) with respect to Equ. (11), we have

$$(1-p)[f'' + f'] = H_p\left[f''' + A1\left(f\, f'' - f'^2 + \frac{A2.A3}{A1} M\,(1-f') + 1 \right)\right] \qquad (28)$$

The zeroth-order equation p^0 of the boundary condition

$$f_0''' + f_0' = 0,\ f_0(0) = S,\ f_0'(0) = \lambda + \alpha\left(1-\beta.f_0''\right)^{-0.5} f_0'' \qquad (29)$$

The solution of the zeroth-order equation as

$$f_0(\xi) = -\frac{e^{-\xi}\left(1 - e^{\xi} + n - ne^{\xi} - \alpha e^{\xi} + \alpha n e^{\xi}\right)}{1+n} \qquad (30)$$

The first-order equation p^1 :

$$f_1''' + f_1' = f_0''' + f_0' + C_1\left[f_0''' + A1\left(f_0\, f_0'' - f_0'^2 + \frac{A2.A3}{A1} M\,(1-f_0') + 1 \right)\right], \qquad (31)$$

$f_1(0) = 0, \quad f_1'(0) = 0$

The second-order equation p^2 :

$$\left\{ \begin{array}{l} f_2''' + f_2' = f_1''' + f_1' + C_1\left[f_1''' + A1\left(f_0\, f_1'' + f_1\, f_0'' - 2 f_0' f_1' - \frac{A2.A3}{A1} M f_1' \right)\right] \\ + C_2\left[f_0''' + A1\left(f_0\, f_0'' - f_0'^2 + \frac{A2.A3}{A1} M\,(1-f_0') + 1 \right)\right], \quad f_2(0) = 0, \quad f_2'(0) = 0 \end{array} \right\} \qquad (32)$$

Solving the Equs. (31) and (32) with the boundary conditions with the help of Equ. (30), then the solution of Equ. (8) can be determined approximately in the form:

$$f(\xi) = f_0(\xi) + f_1(\xi) + f_2(\xi) \qquad (33)$$

Therefore the residual equation become

$$R_1(\xi, C_1, C_2) = \left[f'''(\xi) + A1\left(f(\xi) f''(\xi) - f'^2(\xi) + \frac{A2.A3}{A1} M (1 - f'(\xi)) + 1 \right) \right] \quad (34)$$

The constants C_1 and C_2 can be optimally identified from the conditions:

$$\frac{\partial J_1}{\partial C_1} = \frac{\partial J_1}{\partial C_2} = 0 \quad \text{where} \quad J_1(C_i) = \int_0^\infty R_1^2(\xi, C_i)\, d\xi \quad (35)$$

4.2.Approximation of the energy boundary layer problem

Based on the OHAM, the Equ. (19) with the boundary conditions (14) can be applied as

$$L = g' + g \quad \text{and} \quad N = g'' + \frac{Sc}{A_4}\left(fg' - Kg(1-g)^2 \right) - \left(g' + g \right)$$

L and N - the nonlinear operator. Again by OHAM on Equ. (19) with respect to Eq. (14), we have

$$(1 - p)[g' + g] = H_p \left[g'' + \frac{Sc}{A_4}\left(fg' - Kg\,(1-g)^2 \right) \right] \quad (36)$$

The zeroth-order equation p^0 :

$$\left(g_0' + g_0 \right) = 0, \quad g_0(0) = \frac{A4.g_0'}{Kc} \quad (37)$$

Therefore the solution of zeroth-order equation as

$$\theta_0(\xi) = e^{-\xi} \quad (38)$$

The first-order equation p^1 :

$$g_1' + g_1 = g_0' + g_0 + C_3 \left[g_0'' + \frac{Sc}{A_4}\left(f_0 g_0' - Kg_0(1-g_0)^2 \right) \right], \; g_1(0) = 0 \quad (39)$$

The second-order equation p^2 :

$$\left\{ \begin{array}{c} g_2' + g_2 = g_1' + g_1 + C_3 \left[g_1'' + \frac{Sc}{A_4}\left(f_0 g_1' + f_1 g_0' - Kg_1\left((1-g_0)^2 + 2Kg_0 g_1 \right) \right) \right] \\ + C_4 \left[g_0'' + \frac{Sc}{A_4}\left(f_0 g_0' - Kg_0(1-g_0)^2 \right) \right], \; g_2(0) = 0 \end{array} \right\} \quad (40)$$

Solving the Equs. (39) and (40) with the boundary conditions with the help of Equ. (38), the solution of Equ. (19) can be determined approximately as

$$\theta(\xi) = \theta_0(\xi) + \theta_1(\xi) + \theta_2(\xi) \quad (41)$$

The residual equation becomes

$$R_2(\xi, C_3, C_4) = g''(\xi) + \frac{Sc}{A_4}\left(f(\xi) g'(\xi) - Kg(\xi)(1 - g(\xi))^2 \right) \quad (42)$$

The constants C_3 and C_4 can be optimally derived from

$$\frac{\partial J_2}{\partial C_3} = \frac{\partial J_2}{\partial C_4} = 0 \quad \text{where} \quad J_2(C_i) = \int_0^\infty R_2^2(\xi, C_i)\, d\xi \quad (43)$$

5. Results and Discussion

Calculations are performed by the OHAM method and the numerical method for different values of magnetic parameter, homogeneous and heterogeneous parameter, slip parameter,stretching/shrinking Schmidt number and

the nanoparticle volume fraction. Equations (11)and (19) subjected to the boundary conditions (14) have been solved numerically and analytically for some values of the governing parameters using computer algebra software Maple 18 (Numeric) and Mathematica 5.2 (Analytic). Throughout this calculation we have considered $Sc = 1.0$ corresponds to nanofluids unless otherwise specified. In order to validate our method, we have compared the results of $f''(0)$ with those of wang [11], Bhatacharyya [53] and Abbas [54] and found them in excellent agreement, Table 2.

Table 1: Thermophysical properties of fluid and nanoparticles Chaoli Zhang et al. [52]

	$\rho(kg/m^3)$	$c_p(J/kgK)$	$k(W/mK)$	$\sigma(S/m)$
Pure water	997.1	4179	0.613	5.5×10^{-6}
Copper (Cu)	8933	385	401	59.6×10^{6}
Alumina (Al_2O_3)	3970	765	40	35×10^{6}
SWCNTs	2600	425	6600	101.32×10^{6}

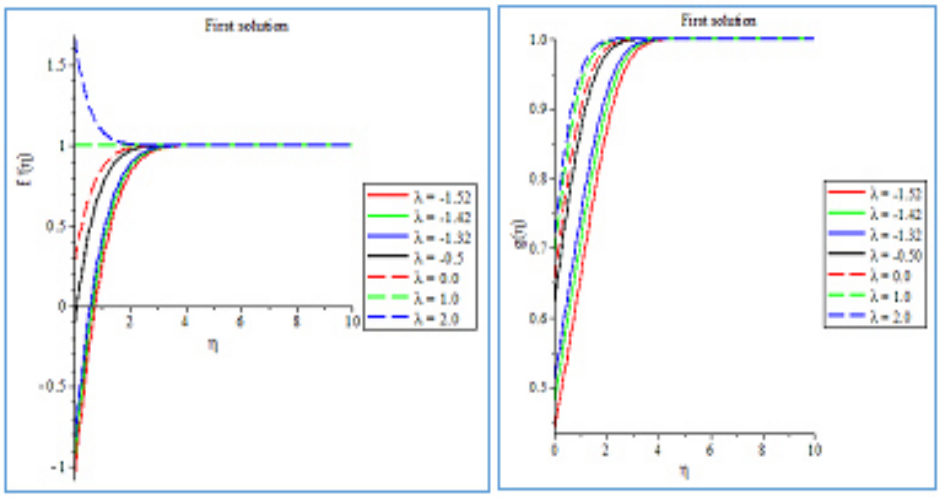

Fig.2: Comparison of velocity and concentration profiles with Mariam and Zaheer [51]

It is predicted from the Fig. 2 that the agreement with the solution of velocity and concentration profile for various values of stretching/shrinking parameter is significantly correlates with Fig. 1 of Mariam and Zaheer [51].

Table2: Comparison of numerical and OHAM values of $f''(0)$ with $S = \alpha = \beta = M = 0.0$

λ	Wang[11]	Bhattacharyya[53]	Abbas et al.[54]	present result	
				Numerical	OHAM
0	1.232588		1.232587	1.23258766	1.23258032
0.1	1.14656		1.146561	1.14656100	1.14656098
0.2	1.05113		1.051129	1.05112999	1.05112992
0.5	0.71330		0.713294	0.71329495	0.71329489
-0.25	1.40224	1.4022405	1.402240	1.40224083	1.40224078
-0.5	1.49567	1.4956697	1.495669	1.49566980	1.49566971
-0.75	1.48930	1.4892981	1.489298	1.48929830	1.48929826
-1.0	1.32882	1.3288169	1.328816	1.32881700	1.32881694

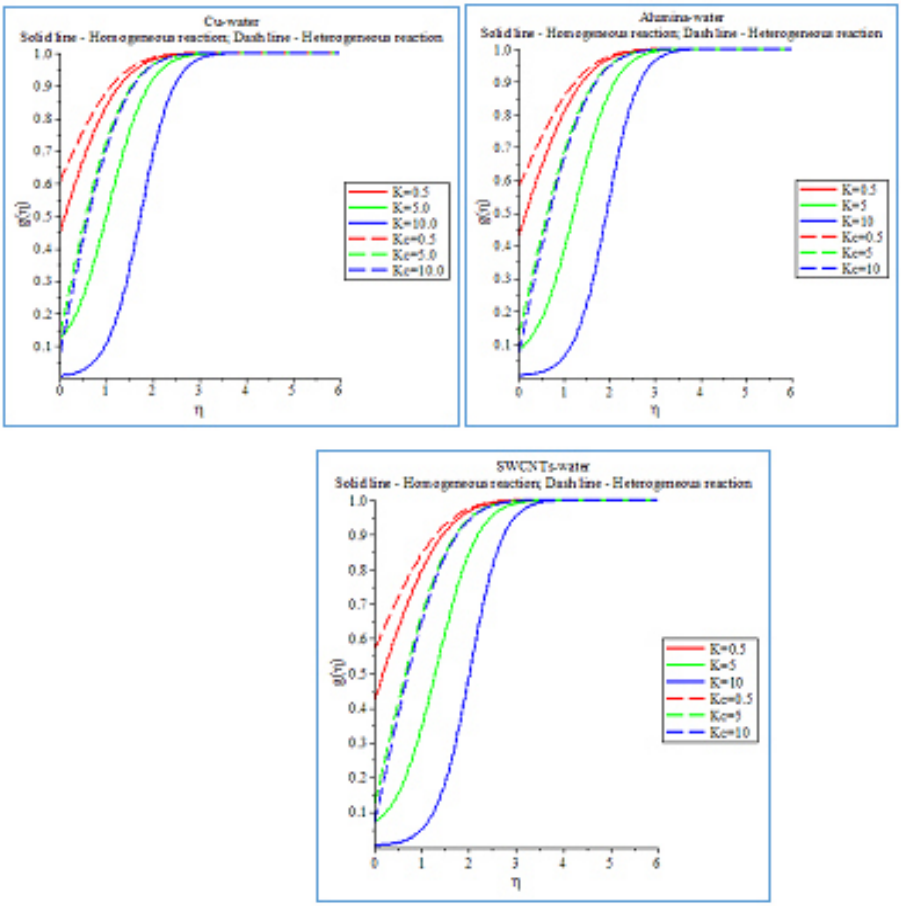

Fig 3: Homogeneous – heterogeneous reactions on concentration profiles

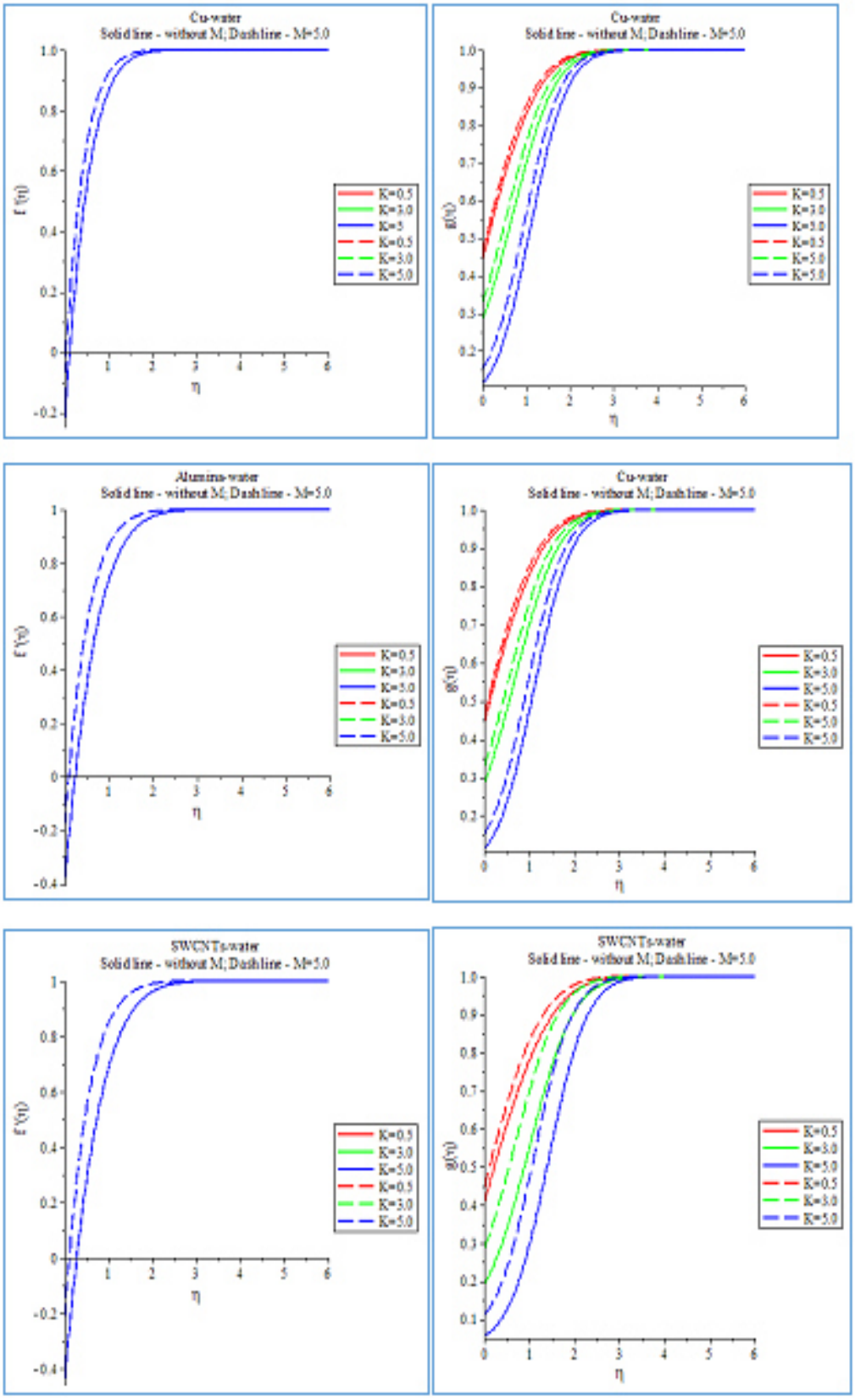

Fig.4: Homogeneous reactions on velocity and concentration profiles

Table3: Value of $-g'(0)$ of K and Kc with $S=0.5, Sc=1.0, \zeta=0.1, \alpha=0.2, \beta=0.3, \lambda=-1.0, M=1.0$

Nanofluid	Homogeneous reaction			Heterogeneous reaction		
	K	Kc	$-g'(0)$	Kc	K	$-g'(0)$
Cu-water	0.5	1.0	-0.4959839	0.5	1.0	-0.3352171
	5.0		-0.1358555	5.0		-0.7240844
	10.0		-0.0088982	10.0		-0.7823376
Al_2O_3-water	0.5	1.0	- 0.4712281	0.5	1.0	- 0.3206595
	5.0		- 0.0910489	5.0		- 0.6623447
	10.0		- 0.0047769	10.0		- 0.7127256
SWCNTs-water	0.5	1.0	- 0.4619637	0.5	1.0	- 0.3149175
	5.0		- 0.0779066	5.0		- 0.6399790
	10.0		- 0.0037578	10.0		- 0.6877162

Table 4: Value of $-g'(0)$ of K with $S=0.5, Sc=1.0, \zeta=0.1, \alpha=0.2, \beta=0.3, \lambda=-1.0, Kc=1.0$

Nanofluid	Homogeneous reaction		
	K	$M=0.0$	$M=5.0$
Cu-water	0.5	-0.4905997	-0.5107121
	3.0	-0.3138822	-0.3621996
	5.0	-0.1251638	-0.1692825
Al_2O_3-water	0.5	- 0.4607455	- 0.4961405
	3.0	- 0.2397028	- 0.3267015
	5.0	- 0.0769082	- 0.1349660
SWCNTs-water	0.5	- 0.4489701	- 0.4911852
	3.0	- 0.2117509	- 0.3142713
	5.0	- 0.0629854	- 0.1245872

Table 5: Value of $-g'(0)$ of Kc with $S=0.5, Sc=1.0, \zeta=0.1, \alpha=0.2, \beta=0.3, \lambda=-1.0, K=1.0$

Nanofluid	Heterogeneous reaction		
	Kc	$M=0.0$	$M=5.0$
Cu-water	0.5	-0.3321455	-0.3433937
	3.0	-0.6497180	-0.6940262
	5.0	-0.7104507	-0.7621699
Al_2O_3-water	0.5	- 0.3141638	- 0.3352922
	3.0	- 0.5859930	- 0.6616713
	5.0	- 0.6371820	- 0.7243347
SWCNTs-water	0.5	- 0.3065798	- 0.3324607
	3.0	- 0.5615432	- 0.6508058
	5.0	- 0.6094139	- 0.7116734

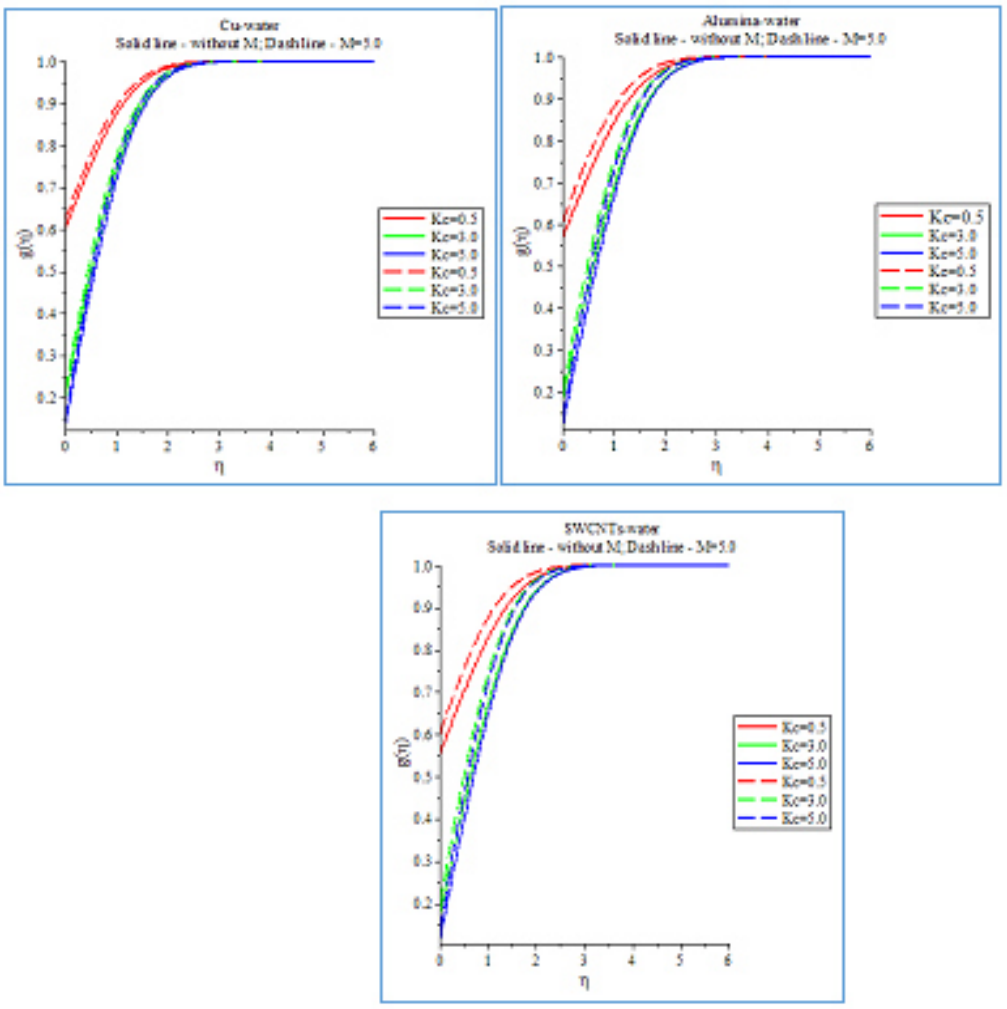

Fig.5: Heterogeneous reactions on concentration profiles

Table 6: Value of $-g'(0)$ of Kc with $M = 5.0, S = 0.5, Sc = 1.0, \zeta = 0.1, \beta = 0.3, \lambda = -1.0, K = 0.0$

Nanofluid		Heterogeneous reaction	
	Kc	$\alpha = 0.0$	$\alpha = 0.2$
Cu-water	0.5	- 0.3244125	- 0.3582453
	3.0	- 0.6319135	- 0.7743634
	5.0	- 0.6837630	- 0.8536915
Al_2O_3-water	0.5	- 0.0166181	- 0.3523986
	3.0	- 0.6080867	- 0.7475542
	5.0	- 0.6559518	- 0.8212233
SWCNTs-water	0.5	- 0.3159493	- 0.3504078
	3.0	- 0.6005773	- 0.7386519
	5.0	- 0.6472221	- 0.8104925

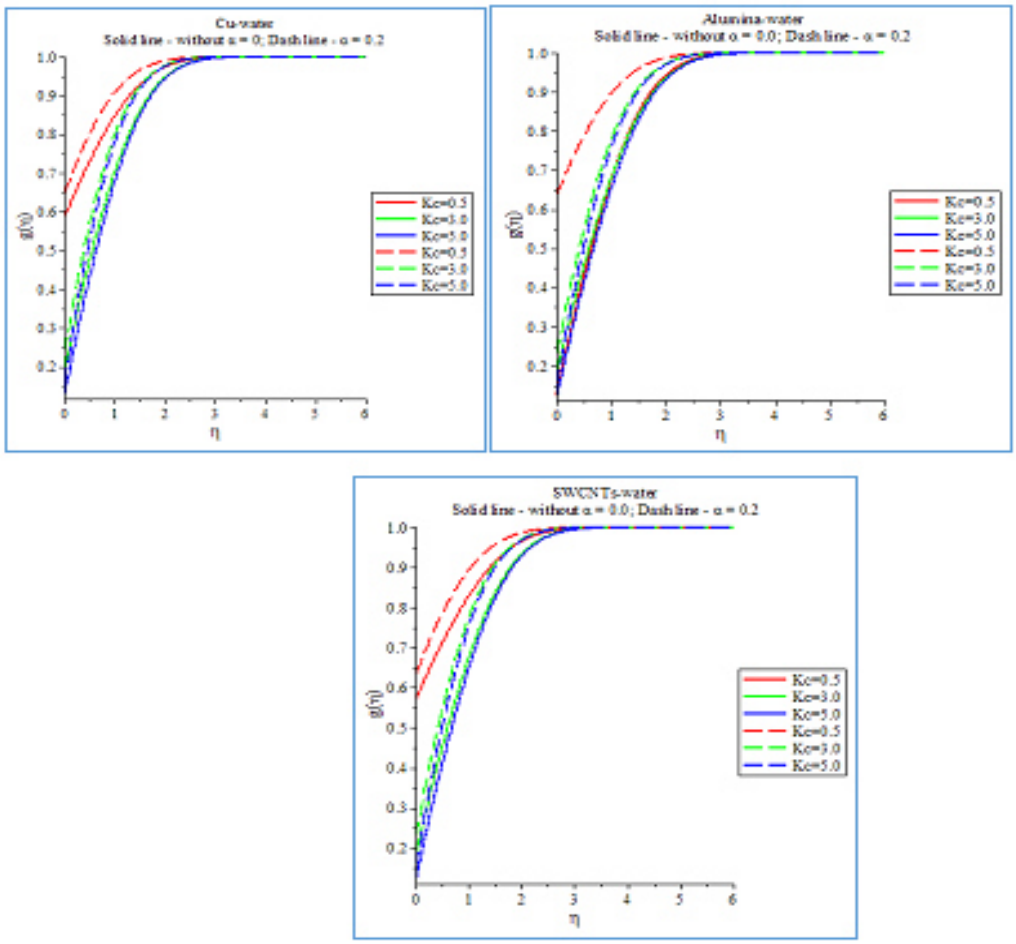

Fig.6: Heterogeneous reactions on concentration profiles in the presence of slip parameter

Table 6: Value of $-g'(0)$ of Kc with $M = 5.0, S = 0.5, Sc = 1.0, \zeta = 0.1, \beta = 0.3, \lambda = -1.0, K = 0.0$

Nanofluid		Heterogeneous reaction	
	Kc	$\alpha = 0.0$	$\alpha = 0.2$
Cu-water	0.5	- 0.3244125	- 0.3582453
	3.0	- 0.6319135	- 0.7743634
	5.0	- 0.6837630	- 0.8536915
Al_2O_3-water	0.5	- 0.0166181	- 0.3523986
	3.0	- 0.6080867	- 0.7475542
	5.0	- 0.6559518	- 0.8212233
SWCNTs-water	0.5	- 0.3159493	- 0.3504078
	3.0	- 0.6005773	- 0.7386519
	5.0	- 0.6472221	- 0.8104925

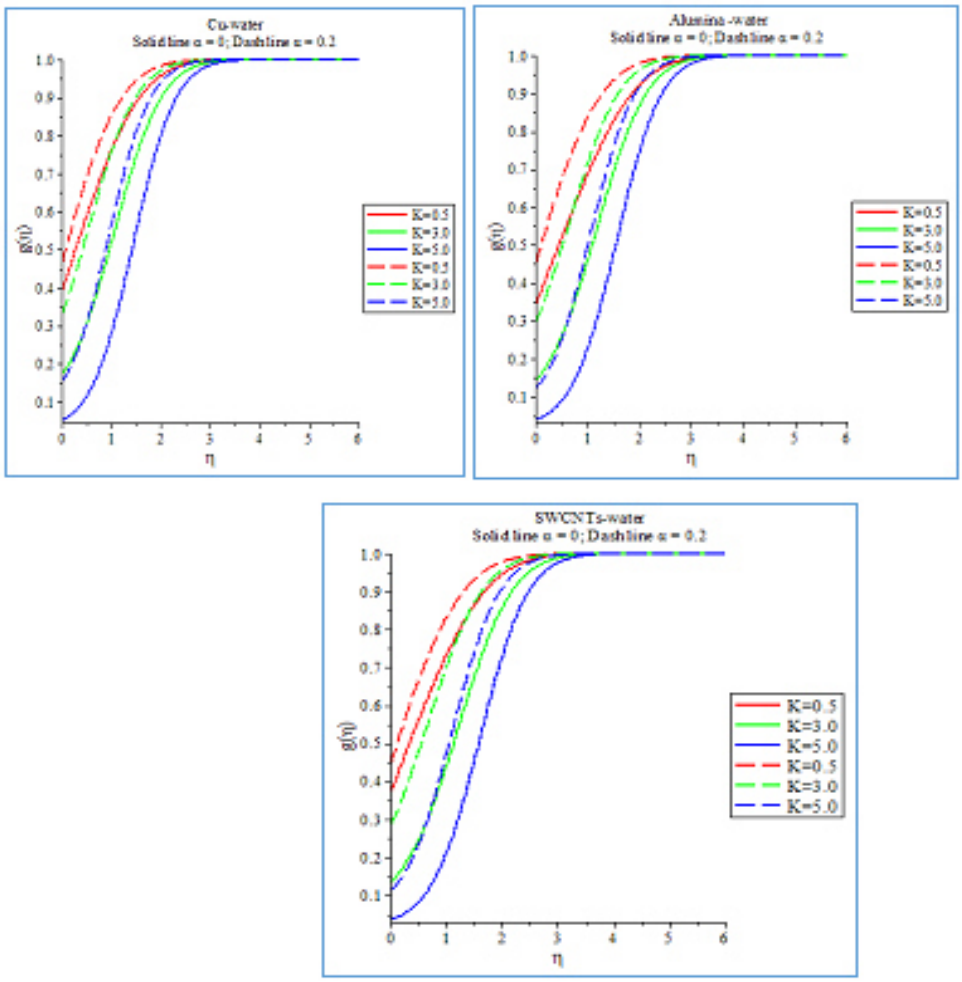

Fig.7: Homogeneous reactions on concentration profiles in the presence of slip parameter

Table 7: Value of $-g'(0)$ of K with $M = 5.0, S = 0.5, Sc = 1.0, \zeta = 0.1, \beta = 0.3, \lambda = -1.0, Kc = 1.0$

Nanofluid		Homogeneous reaction	
	K	$\alpha = 0.0$	$\alpha = 0.2$
Cu-water	0.5	- 0.4285015	- 0.5107060
	3.0	- 0.1874988	- 0.3621771
	5.0	- 0.0567523	- 0.1692386
Al_2O_3-water	0.5	- 0.3765418	- 0.4961307
	3.0	- 0.1570446	- 0.3266626
	5.0	- 0.0436761	- 0.1349028
SWCNTs-water	0.5	- 0.4077608	- 0.4911737
	3.0	- 0.1479059	- 0.3142244
	5.0	- 0.0400412	- 0.1245158

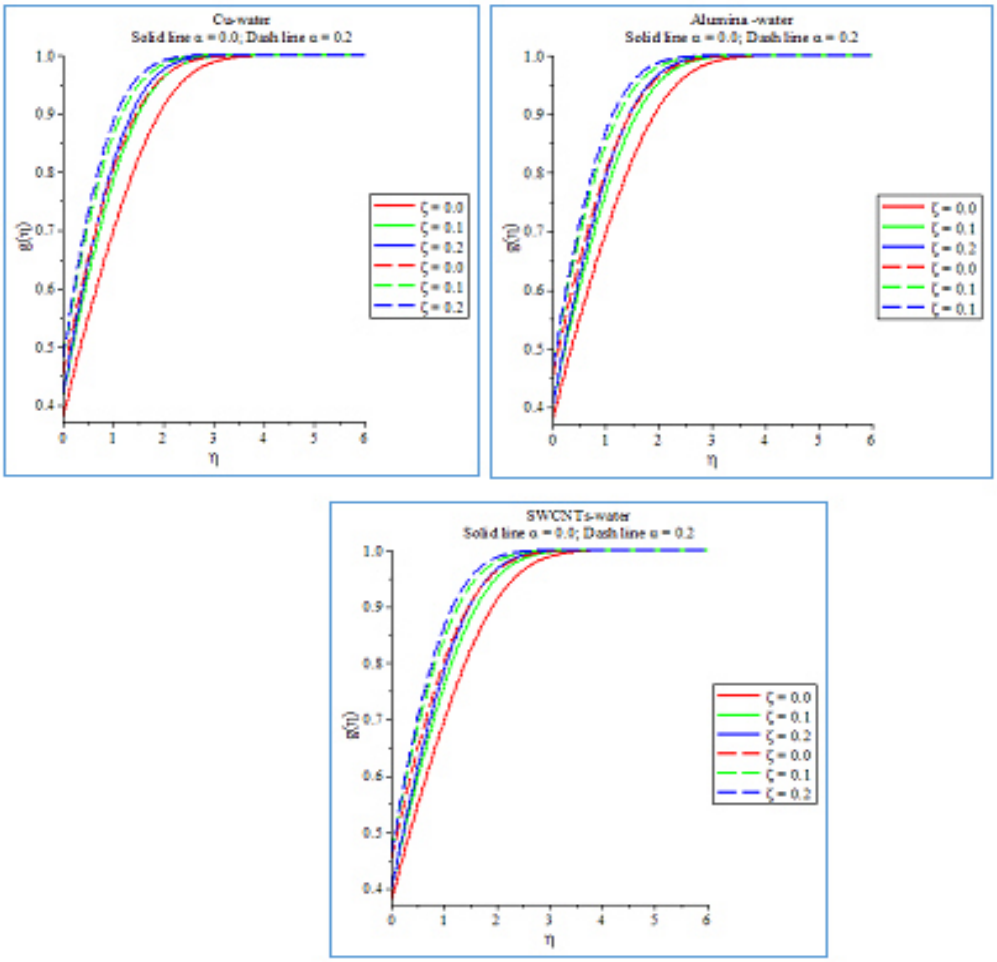

Fig.8: Nanoparticle volume fraction on concentration profiles in the presence of slip parameter with heterogeneous reaction

Table 8: Value of $-g'(0)$ of ζ with $M = 5.0, S = 0.5, Sc = 1.0, K = 0.0, \beta = 0.3, \lambda = -1.0, Kc = 1.0$

Nanofluid	ζ	Heterogeneous reaction $\alpha = 0.0$	$\alpha = 0.2$
Cu-water	0.0	- 0.3756943	- 0.4478159
	0.1	- 0.4581912	- 0.5287135
	0.2	- 0.5145962	- 0.5918442
Al_2O_3-water	0.0	- 0.3756943	- 0.4478159
	0.1	- 0.4455330	- 0.5160769
	0.2	- 0.4987162	- 0.5761351
SWCNTs-water	0.0	- 0.3756943	- 0.4478159
	0.1	- 0.4414885	- 0.5118185
	0.2	- 0.4935427	- 0.5706037

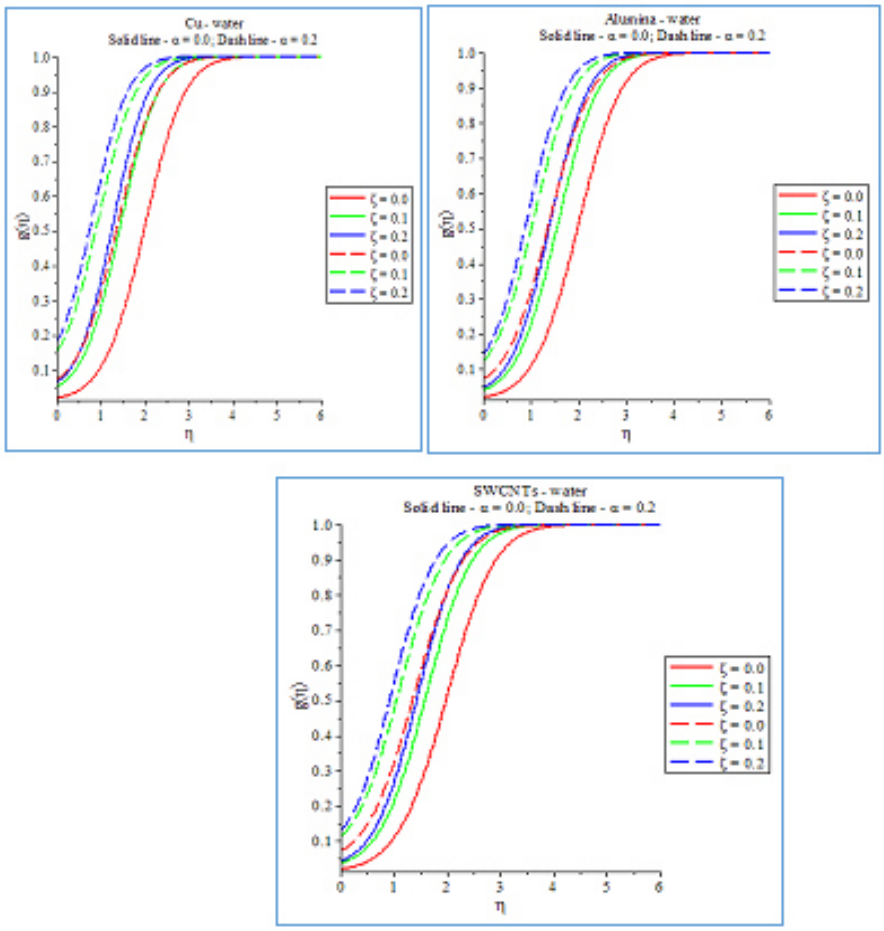

Fig.9: Nanoparticle volume fraction on concentration profiles in the presence of slip parameter with homogeneous reaction

Table 9: Value of $-g'(0)$ of ζ with $M = 5.0, S = 0.5, Sc = 1.0, K = 5.0, \beta = 0.3, \lambda = -1.0, Kc = 1.0$

Nanofluid	ζ	Homogeneous reaction $\alpha = 0.0$	$\alpha = 0.2$
Cu-water	0.0	- 0.0187644	- 0.0713608
	0.1	- 0.0567523	- 0.1692386
	0.2	- 0.0777319	- 0.2224368
Al_2O_3-water	0.0	- 0.0187644	- 0.0713608
	0.2	- 0.0436761	- 0.1349028
	0.2	- 0.0578153	- 0.1742693
SWCNTs-water	0.0	- 0.0187644	- 0.0713608
	0.1	- 0.0400412	- 0.1245158
	0.2	- 0.0522299	- 0.1589195

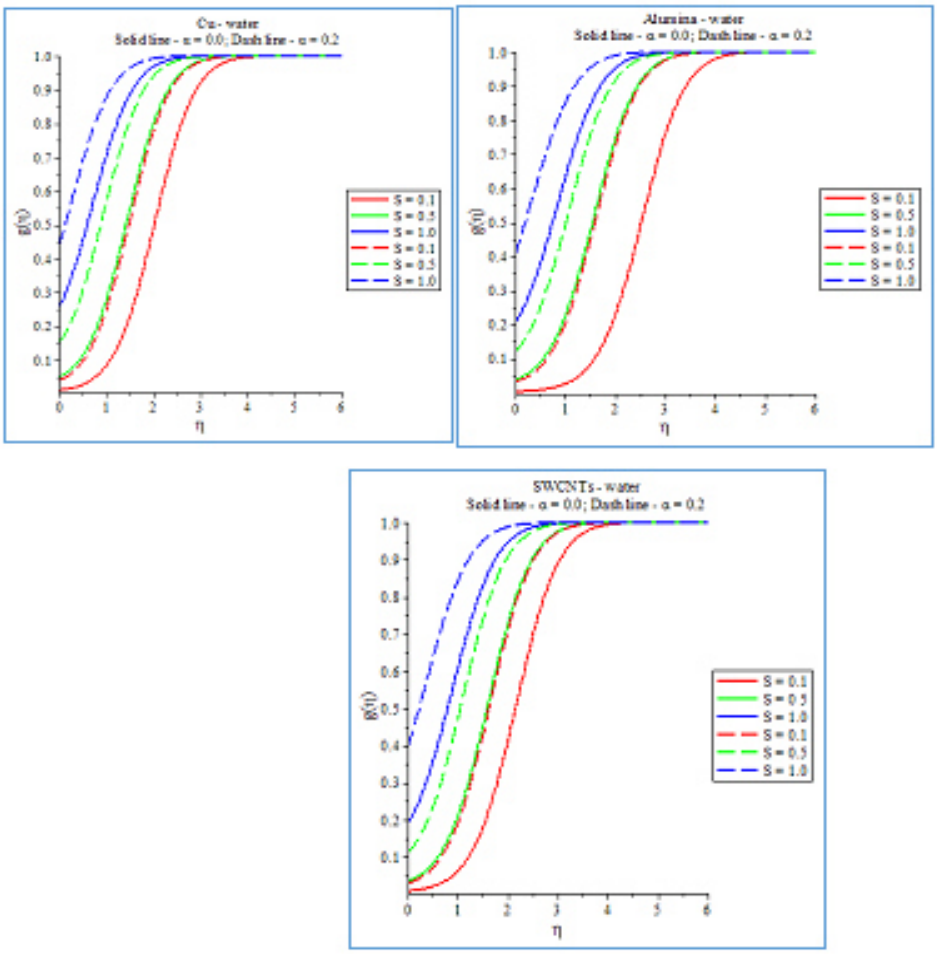

Fig.10: Suction effects on concentration profiles in the presence of slip parameter with homogeneous reaction

Table 10: Value of $-g'(0)$ of S with $M = 5.0, \zeta = 0.1, Sc = 1.0, K = 5.0, \beta = 0.3, \lambda = -1.0, Kc = 1.0$

Nanofluid	S	Homogeneous reaction $\alpha = 0.0$	$\alpha = 0.2$
Cu-water	0.0	- 0.0122590	- 0.0459533
	0.1	- 0.0567523	- 0.1692386
	0.2	- 0.2836026	- 0.4849162
Al_2O_3-water	0.0	- 0.0035430	- 0.0358247
	0.2	- 0.0436761	- 0.1349028
	0.2	- 0.2286255	- 0.4504160
SWCNTs-water	0.0	- 0.0089460	- 0.0329624
	0.1	- 0.0400412	- 0.1245158
	0.2	- 0.2114921	- 0.4367594

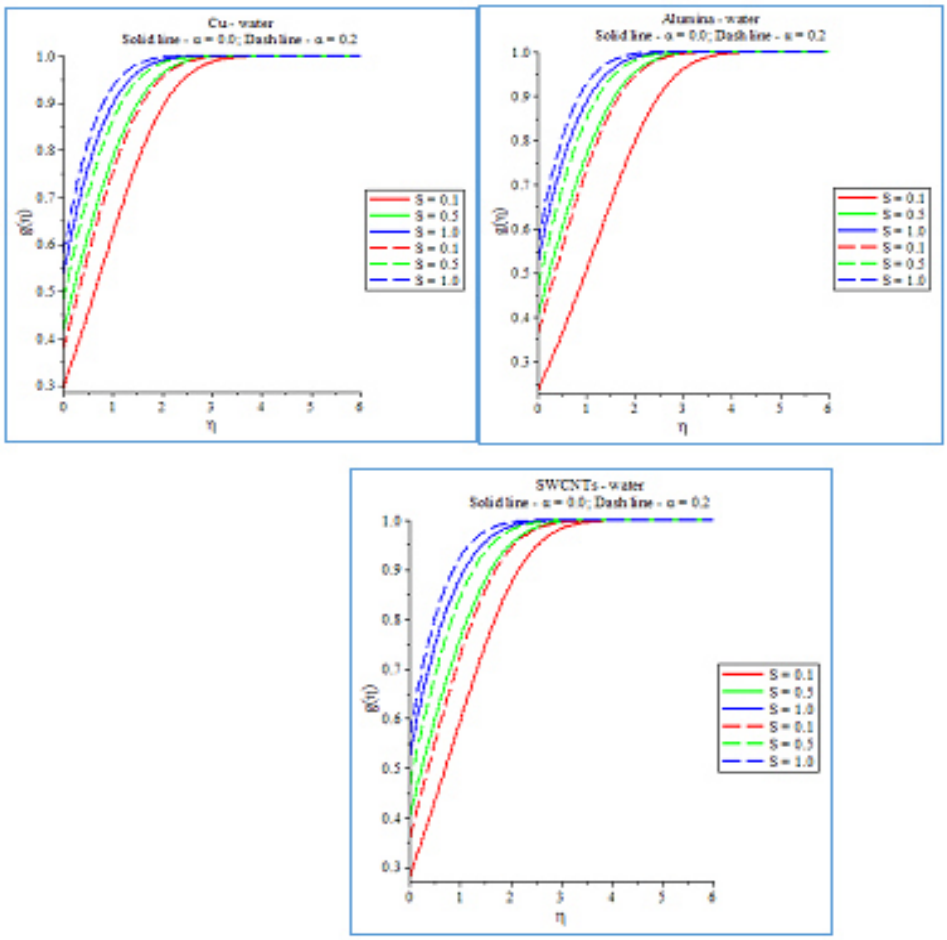

Fig.11: Suction effects on concentration profiles in the presence of slip parameter with heterogeneous reaction

Table 11: Value of $-g'(0)$ of S with $M = 5.0, \zeta = 0.1, Sc = 1.0, K = 0.0, \beta = 0.3, \lambda = -1.0, Kr = 1.0$

Nanofluid		Heterogeneous reaction	
	S	$\alpha = 0.0$	$\alpha = 0.2$
Cu-water	0.0	- 0.3226681	- 0.4141491
	0.1	- 0.4581912	- 0.5287135
	0.2	- 0 .588682	- 0.6355776
Al_2O_3-water	0.0	- 0.2580273	- 0.3997047
	0.2	- 0.4455330	- 0.5160769
	0.2	- 0.5787753	- 0.6267347
SWCNTs-water	0.0	- 0.3070789	- 0.3950418
	0.1	- 0.4414885	- 0.5118185
	0.2	- 0.5755443	- 0.6236029

Figs. 3 shows that the concentration profiles of the water based Cu, Al_2O_3 and SWCNTs in the presence of homogeneous and heterogeneous reaction. It is observed that the concentration of the nanofluids decreases with

increase of homogeneous and heterogeneous reaction while the diffusion boundary layer thickness for homogeneous reaction is stronger than heterogeneous reaction. It is interesting to note that the concentration of the water based Cu, Al_2O_3 and SWCNTs decreases and the rate of mass transfer of the nanofluids increases with increase of homogeneous reaction (exist the mechanism of diffusion properties) whereas the concentration and the rate of mass transfer of the nanofluids decreases with increase of heterogeneous reaction (abnormal to the mechanism of diffusion properties), Fig. 3 and Table 3. Both the homogeneous and heterogeneous reaction, it is also noticed that the rate of mass transfer of SWCNTs - water is stronger as compare with the water based Cu and Al_2O_3 because of the strength of density of the SWCNTs is lower than Cu and Al_2O_3, Table 1.

Both $M = 0.0$ and $M = 5.0$, it is predicted that the concentration of the nanofluids decreases and the rate of mass transfer of the nanofluids (water based Cu, Al_2O_3 and SWCNTs) increases with increase of homogeneous reaction,Fig. 4and Table 4 whereas the concentration and the rate of mass transfer of the nanofluids (water based Cu, Al_2O_3 and SWCNTs) decreases with increase of heterogeneous reaction, Fig. 5 and Tables 5. Both homogeneous and heterogeneous reaction, it is important to note that the concentration of the SWCNTs – water of $M = 5.0$ is stronger than $M = 0.0$ whereas rate of mass transfer decreases with increase of magnetic strength.

In the presence of $\alpha = 0.0$ and $\alpha = 0.2$, it is noticed that the concentration of the nanofluids decreases and the rate of mass transfer of the nanofluids (water based Cu, Al_2O_3 and SWCNTs) increases with increase of homogeneous reaction,Fig. 6and Table 7 whereas the concentration and the rate of mass transfer of the nanofluids (water based Cu, Al_2O_3 and SWCNTs) decreases with increase of heterogeneous reaction, Fig. 7 and Tables 7. Both homogeneous and heterogeneous reaction, it is noted that the diffusion boundary layer thickness of the SWCNTs – water of $\alpha = 0.2$ is higher than $\alpha = 0.0$ whereas rate of mass transfer decreases with increase of slip parameter.

In the presence of $\alpha = 0.0$ and $\alpha = 0.2$, it is interesting to predict that the concentration of water based Cu and SWCNTs is stronger than Al_2O_3– water for heterogeneous reaction whereas the concentration of water based Al_2O_3 and SWCNTs is stronger than Cu– water for homogeneous reaction.It is observed that the concentration of the nanofluids increases and the rate of mass transfer of the nanofluids (water based Cu, Al_2O_3 and SWCNTs) decreases with increase of nanoparticle volume fraction(exist the mechanism of diffusion properties) in the presence of homogeneous and heterogeneous reaction, Figs. 8and 9 and Tables 8 and 9. Both homogeneous and heterogeneous reaction, it is noted that the diffusion boundary layer thickness of the SWCNTs – water of $\alpha = 0.2$ is higher than $\alpha = 0.0$ with increase of the nanoparticle volume fraction.In the presence of heterogeneous and homogeneous reaction with slip factor, it is important to observe that the rate of mass transfer of water based SWCNTs – water is stronger than the water based Cu and Al_2O_3– water, Tables 8 and 9.

The concentration of the nanofluids increases and the rate of mass transfer of the nanofluids (water based Cu, Al_2O_3 and SWCNTs) decreases with increase of suction in the presence of homogeneous and heterogeneous reaction, Figs. 10and 11 and Tables 10 and 11. Both homogeneous and heterogeneous reaction, it is found that the concentration of the SWCNTs – water of $\alpha = 0.2$ is higher than $\alpha = 0.0$ with increase of suction.In the presence of heterogeneous and homogeneous reaction with slip factor, it is important to note that the rate of mass transfer of water based SWCNTs – water is stronger than the water based Cu and Al_2O_3– water, Tables 10 and 11. It is also observed that the diffusion boundary layer thickness of homogeneous reaction is stronger as compare with heterogeneous reaction.

6. Conclusion

The outcome of generalized homogenous–heterogeneous reactions of the water based Cu, Al_2O_3 and SWCNTs on the boundary layer MHD stagnation point flow over a stretching/shrinking sheet with slip and uniform suction are investigated. The dimensionless governing ODEs of the problem are solved numerically and analytically usingfourth or fifth order Runge-Kutta Fehlberg method with shooting technique and OHAM. The importance of involving parameters on velocity and concentration profiles are graphically illustrated and analyzed in detail. The capital finding of this investigation can be summarized as:

- The concentration of the nanofluids (water based Cu, Al_2O_3 and SWCNTs) decreases with increase of homogeneous and heterogeneous reaction while the diffusion boundary layer thickness for heterogeneous reaction is stronger than homogeneous reaction.
- It is interesting to note that the concentration of the nanofluids decreases and the rate of mass transfer of the water based Cu, Al_2O_3 and SWCNTs increases with increase of homogeneous reaction (exist the mechanism of diffusion properties) whereas the concentration and the rate of mass transfer of the

nanofluids decreases with increase of heterogeneous reaction (abnormal to the mechanism of diffusion properties) in the presence of magnetic field and slip parameter.

- The concentration and the rate of mass transfer of the SWCNTs - water is stronger as compare with the water based Cu and $Al_2O_3$with increase of homogeneous and heterogeneous reaction and suction of the surface in the presence of magnetic field and slip parameter whereas the rate of mass transfer of the nanofluids decreases with increase of magnetic strength and slip parameter.
- It is important to predict that the concentration of the nanofluids increases and the rate of mass transfer of the water based Cu, Al_2O_3 and SWCNTs decreases with increase of nanoparticle volume fractionand suction parameter (exist the mechanism of diffusion properties) in the presence of homogeneous and heterogeneous reaction with slip parameter. The diffusion boundary layer thickness for $\alpha = 0.2$ is higher than $\alpha = 0.0$ with increase of nanoparticle volume fraction and suction of the surface in the presence of homogeneous and heterogeneous reaction with slip factor of the surface.
- Homogeneous reaction on the water based Cu, Al_2O_3 and SWCNTs agree the physical significance of diffusion properties as comparedto the heterogeneous reaction.

Reactions which are significantly affected by mass transfer of water based Cu, Al_2O_3 and SWCNTs are called mass-transfer limited or diffusion-limited reactions. It is also possible to distinguish the relative influence of internal and external mass transfer. Improvement of mass transfer of SWCNTs-water and the elimination of mass-transfer limitations are desired objectives in heterogeneous reactions as compared to the other mixture in the flow region.

Nomenclature

B_0	Magnetic flux density, $kg\,s^{-2}A^{-1}$
a	Concentration of the chemical species A, K
b	Concentration of the chemical species B, K
$(D_A)_f$	Specific Diffusivity of the chemical species A, $m^2\,s^{-1}$
$(D_B)_f$	Specific Diffusivity of the chemical species B, $m^2\,s^{-1}$
$(D_A)_{nf}$	Specific Diffusivity of the chemical species A in base fluid, $m^2\,s^{-1}$
$(D_B)_{nf}$	Specific Diffusivity of the chemical species B in base fluid, $m^2\,s^{-1}$
K_h, K_s	First order rate of heterogeneous and homogeneous reaction, s^{-1}
M	Magnetic parameter, $\frac{B_0^2\sigma_f x}{\rho_f u_e}$, $\left(\frac{\Omega^{-1}m^{-1}B_0^2\,m}{m\,s^{-1}\,kg\,m^{-3}}\right)$ (-)
Re	Reynolds number, $\frac{u_e x}{\nu_f}$, $\frac{m\,s^{-1}m}{m^2 s^{-1}}$ (-)
Sc	Schmidt number, $\frac{\nu_f}{(D_A)_f}$, $\frac{m^2\,s^{-1}}{m^2\,s^{-1}}$ (-)
x, y	Stream-wise coordinate and cross-stream coordinate, m
u, v	Velocity components in x and y direction, $m\,s^{-1}$
u_w, u_e	Flow velocity of the fluid away from the plate, $m\,s^{-1}$

Greek symbols

ρ_f	Density of the base fluid, $kg\ m^{-3}$
ρ_s	Density of the nanoparticle, $kg\ m^{-3}$
ρ_{nf}	Effective density of the nanofluid, $kg\ m^{-3}$
σ	Electric conductivity, $\Omega^{-1}m^{-1}$
μ_f	Dynamic viscosity of the base fluid, $kg\ m^{-1}\ s^{-1}$
μ_{nf}	Effective dynamic viscosity of the nanofluid, $kg\ m^{-1}\ s^{-1}$
K	Homogeneous reaction parameter, $\frac{K_h a_0^2 x}{u_e}, \frac{s^{-1}m^2}{m^2\ s^{-1}}$ (-)
K_c	Heterogeneous reaction parameter, $= \frac{K_s \mathrm{Re}^{-0.5}}{(D_A)_f}, \frac{s^{-1}m^2}{m^2\ s^{-1}}$ (-)
ν_f	Dynamic viscosity of the nanofluid, $m^2\ s^{-1}$
ζ	Nanoparticle volume fraction,(-)
ψ	Dimensionless stream function, (-)
η	Similarity variable, (-)
f	Dimensionless stream function, (-)

Acknowledgement: The authors wish to express their cordial thanks to our beloved The Vice Chancellor and The Dean, FSTPi, UTHM, Malaysia for their encouragements and acknowledge the financial support received from IGSP/U255/UTHM /2014.

References

1. K. Heimenz, Die Grenzschicht an einem in den gleichförmingen Flussigkeitsstorm eingetauchten graden Kreiszylinder, Dinglers Polytech J, 326 (1911) 321–324.
2. J. Paullet, P. Weidman, Analysis of stagnation point flow toward a stretching sheet, Int J Non-Linear Mech., 42 (2007) 1084–1091.
3. P.R. Sharma, G. Singh, Effects of variable thermal conductivity and heat source/ sink on MHD flow near a stagnation point on a linearly stretching sheet, J Appl. Fluid Mech., 2 (2009) 13–21.
4. A. Ishak, K. Jafar, R. Nazar, I. Pop, MHD stagnation point flow towards a stretching sheet, Physica A, 388 (2009) 3377–3383.
5. T. Hayat, Z. Abbas, I. Pop, S. Asghar, Effects of radiation and magnetic field on the mixed convection stagnation-point flow over a vertical stretching sheet in a porous medium, Int J Heat Mass Transfer, 53 (2010) 466–474.
6. F.M. Ali, R. Nazar, N.M. Arifin, I. POP, MHD stagnation-point flow and heat transfer towards stretching sheet with induced magnetic field, Appl. Math Mech. Engl. Ed, 32 (2011) 409–418.
7. S.V. Subhashini, R. Sumathi, I. Pop, Dual solutions in a double-diffusive convection near stagnation point region over a stretching vertical surface, Int. J Heat Mass Transfer, 55 (2012) 2524–2530.
8. K. Bhattacharyya, S. Mukhopadhyay, G.C. Layek, Reactive solute transfer in magnetohydrodynamic boundary layer stagnation-point flow over a stretching sheet with suction/blowing, Chem. Eng. Commun,199 (2012) 368–383.
9. N.S. Al-Sudais, Thermal radiation effects on MHD fluid flow near stagnation point of linear stretching sheet with variable thermal conductivity, Int. Math Forum, 7 (2012) 2525–2544.

10. M. Miklavcic, C.Y. Wang, Viscous flow due to a shrinking sheet, Quart Appl. Math., 64 (2006) 283–290.
11. C.Y. Wang, Stagnation flow towards a shrinking sheet, Int. J Nonlinear Mech., 43 (2008) 377–382.
12. K. Bhattacharyya, G.C. Layek, Effects of suction/blowing on steady boundary layer stagnation-point flow and heat transfer towards a shrinking sheet with thermal radiation, Int. J Heat Mass Transfer, 54 (2011) 302–307.
13. K. Bhattacharyya, K. Vajravelu, Stagnation-point flow and heat transfer over an exponentially shrinking sheet, Commun Nonlinear Sci. Numer. Simul., 17 (2012) 2728–2734.
14. M. Ashraf, S. Ahmad, Radiation effects on MHD axisymmetric stagnation point flow towards a heated shrinking sheet, Chem. Eng. Commun., 17 (2012) 823–837.
15. A.M. Rohni, S. Ahmad, I. Pop, Flow and heat transfer at a stagnation point over an exponentially shrinking vertical sheet with suction, Int. J Therm. Sci., 75 (2014) 164–170.
16. S.H.M. Saleh, N.M. Arifin, R. Nazar, F.M. Ali, I. Pop, Mixed convection stagnation flow towards a vertical shrinking sheet, Int. J Heat Mass Transfer, 73 (2014) 839–848.
17. Navier HMLC., Memoires de I'Academie Royale des Sciences de I'Intstitue de France. 1823;6:389.
18. J.C. Maxwell, On Stresses in rarified gases arising from inequalities of temperature, Phil Trans R SocLond, 170 (1879) 231.
19. C.Y. Wang, Flow due to a stretching boundary with partial slip: an exact solution of Navier-Stokes equations, Chem. Eng. Sci. Acta Mech., 57 (2002) 3745–3747.
20. P.A. Thompson, S.M. Troian, A general boundary condition for liquid flow at solid surfaces, Nature, 389 (1997) 360.
21. M.T. Mathews, J.M. Hill, Newtonian flow with nonlinear Navier boundary condition, Acta Mech., 191 (2007) 195.
22. C.Y. Wang, Analysis of viscous flow due to a stretching sheet with surface slip and suction, Nonlinear Anal: Real World Appl., 10 (2009) 375–380.
23. M. Sajid, N. Ali, Z. Abbas, T. Javed, Stretching flows with general slip boundary condition, IntJ Modern Phys B, 24 (2010) 5939–5947.
24. Heterogeneous Mixtures, in chemistry, is where certain elements are unwillingly combined and, when given the option, will separates completely. "Webster's Revised Unabridged Dictionary (1913 + 1828)" (Part of this paragraph is public domain material copyright 1828 and 1913). Heterogeneity. The ARTFL Project, University of Chicago. September 2010. Retrieved 2010-09-10.
25. Jump up to"Webster's Revised Unabridged Dictionary (1913 + 1828)" (Part of this paragraph is public domain material copyright 1828 and 1913). Heterogeneous. The ARTFL Project, University of Chicago. September 2010. Retrieved 2010-09-10.
26. Jump up to "Webster's Revised Unabridged Dictionary (1913 + 1828)" (This is public domain material copyright 1828 and 1913). Homogeneous. The ARTFL Project, University of Chicago. September 2010. Retrieved 2010-09-10.
27. M.A. Chaudhary, J.H. Merkin, A simple isothermal model for homogeneous-heterogeneous reactions in boundary-layer flow. I. Equal Diffusivities, Fluid Dyn Res, 16 (1995) 311–333.
28. M.A. Chaudhary, J.H. Merkin, A simple isothermal model for homogeneous-heterogeneous reactions in boundary-layer flow. I. Diff diffusivities, Fluid Dynamic Res., 16 (1995) 335–359.
29. M.A. Chaudhary, J.H. Merkin, Homogeneous–heterogeneous reactions in boundary-layer flow: effects of loss of reactant, M&L Comput Model, 24 (1996) 21–28.
30. J.H. Merkin, A model for isothermal homogeneous–heterogeneous reactions in boundary-layer flow, Math Comput Model, 24 (1996) 125–136.
31. W.A. Khan, I. Pop, Flow near the two-dimensional stagnation - point on an infinite permeable wall with a homogeneous–heterogeneous reaction, Commun Nonlinear Sci. Numer Simul, 15 (2010) 3435–3443.
32. N. Bachok, A. Ishak, I. Pop, On the stagnation-point flow towards a stretching sheet with homogeneous–heterogeneous reactions effect, Commun Nonlinear Sci. Numer Simul, 16 (2011) 4296–4302.
33. W.A. Khan, I. Pop, Effects of homogeneous–heterogeneous reactions on the viscoelastic fluid toward a stretching sheet, J Heat Mass Transfer, 134 (2012) 064506–064601.
34. P.K. Kameswaran, S. Shaw, P. Sibanda, P.V.S.N. Murthy, Homogeneous-heterogeneous reactions in a nanofluid flow due to a porous stretching sheet, Int. J Heat Mass Transfer, 57 (2013) 465–472.
35. P.K. Kameswaran, P. Sibanda, C. RamReddy, P.V.S.N. Murthy, Dual solutions of stagnation-point flow of a nanofluid over a stretching surface, Boundary Value Probl, 2013 (2013) 188.

36. S. Shaw, P.K. Kameswaran, P. Sibanda, Homogeneous–heterogeneous reactions in micropolar fluid flow from a permeable stretching or shrinking sheet in a porous medium, Boundary Value Probl, 2013 (2013) 77.
37. Liu, K.V., Choi, U.S., Kasza, K.E., 1988. Measurements of pressure drop and heat transfer in turbulent pipe flows of particulate slurries. Argonne Nantional Laboratory Report, ANL-88-15
38. A.S. Ahuja, Augmentation of heat transfer in laminar flow of polystyrene suspensions, J. Appl. Phys., 46 (1975) 3408–3425.
39. Eastman, J.A., Choi, U.S., Li, S., Thompson, L.J., Lee, S., 1997. Enhanced thermal conductivity through the development of nanofluids. In: Komarneni, S., Parker, J.C., Wollenberger, H.J. (Eds.), Nanophase and Nanocomposite Materials II. MRS, Pittsburg, PA, pp. 3–11
40. U.S. Choi, Enhancing thermal conductivity of fluids with nanoparticles, ASME FED, 231 (1995) 99–103.
41. Das, S. K., Putra, N., Thiesen, P. and Roetzel, W., Temperature Dependence of Thermal Conductivity Enhancement for Nanofluids. Transactions of ASME, Journal of Heat Transfer, vol. 125 (2003) 567–574.
42. Lee, S., Choi, S. U. S., Li, S. and Eastman, J. A., Measuring Thermal Conductivity of Fluids Containing Oxide Nanoparticles. Transactions of ASME, Journal of Heat Transfer, vol. 121(1999) 280–289.
43. Bhattacharya, P., Saha, S. K., Yadav, A., Phelan, P. E. and Prasher, R. S., Brownian Dynamics Simulation to Determine the Effective Thermal Conductivity of Nanofluids. Journal of Applied Physics, vol. 95 (2004) 6492–6494.
44. Xuan, Y. and Yao, Z. 2005. 2004, Lattice Boltzmann Model for Nanofluids. Heat and Mass Transfer, 41 (2004) 199–205.
45.Nan, C. W., Shi, Z. and Lin, Y., A Simple Model for Thermal Conductivity of Carbon Nanotube-Based Composites. Chemical Physics Letters, 375(2003) 666–669.
46. Maxwell-Garnett, J. C., Colours in Metal Glasses and in Metallic Films. Philosophical Transactions of the Royal Society of London, Series A, 203(1904) 385–420.
47. Aziz, A., Similarity solution for laminar thermal boundary layer over a flat plate with a convective surface boundary condition, Commun. Nonlinear Sci. Numer Simul., 14 (2009) 1064-1068.
47.Nan, C. W., Liu, G., Lin, Y. and Li, M., Interface Effect on Thermal Conductivity of Carbon Nanotube Composites. Applied Physics Letters, vol. 85(2004) 3549–3551.
48. Sivasankaran Harish, Kei Ishikawa, Erik Einarsson, Shinya Aikawa, ShoheiChiashi, Junichiro Shiomi, Shigeo Maruyama, Enhanced thermal conductivity of ethylene glycol with single-walled carbon nanotube inclusions, International Journal of Heat and Mass Transfer, 55 (2012)3885–3890.
49. Mohamed Abd El-Aziz, Dual solutions in hydromagnetic stagnation point flow and heat transfer towards a stretching/shrinking sheet with non-uniform heat source/sink and variable surface heat flux, Journal of the Egyptian Mathematical Society, Available online 18 November 2015.
50. V. Marinca, N. Herisanu, Application of optimal homotopy method for solving nonlinear equations arising in heat transfer, Int. Commun. Heat Mass Transfer 35 (2008) 710-715.
51. Mariam Sheikh and Zaheer Abbas, Homogeneous-heterogeneous reactions in stagnation point flow of Casson fluid due to a stretching/shrinking sheet with uniform suction and slip effects, Ain Shams Engineering Journal, 2015, Article in press.
52. Chaoli Zhang, Liancun Zheng, Xinxin Zhang and Goong Chen, MHD flow and radiation heat transfer of nanofluids in porous media with variable surface heat flux and chemical reaction, Applied Mathematical modelling, 39(2015) 165-181.
53. K. Bhattacharyya, Dual solutions in boundary layer stagnation-point flow and mass transfer with chemical reaction past a stretching/shrinking sheet, Int. Commun Heat Mass Transfer, 38 (2011) 917–922.
54. Z. Abbas, M. Sheikh, I. Pop, Stagnation-point flow of a hydromagnetic viscous fluid over stretching/shrinking sheet with generalized slip condition in the presence of homogeneous–heterogeneous reactions, Journal of the Taiwan Institute of Chemical Engineers, 55 (2015), 69 –75.
55. E. Magyari, Comment on the homogeneous nanofluid models applied to convective heat transfer problems, Acta Mech., 222 (2011) 381–385.
56. E. Mamut, Characterization of heat and mass transfer properties of nanofluids, Rom. J. Phys., 51 (2006) 5–12.